# Solvation-Protection-Enabled High-Voltage Electrolyte for Lithium Metal Batteries

Chi-Cheung Su,[a*] Meinan He,[b] Mei Cai,[b] Jiayan Shi,[a,c] Rachid Amine,[d] Nancy Dietz Rago,[a] Juchen Guo,[c] Tomas Rojas,[d,e] Anh T. Ngo,[d,e] and Khalil Amine[a,f*]

[a] Chemical Sciences and Engineering Division, Argonne National Laboratory, 9700 S. Cass Avenue, Lemont, IL 60439, USA

[b] General Motors Global Research and Development Center, 30500 Mound Road, Warren, MI 48090, USA

[c] Department of Chemical and Environmental Engineering, University of California-Riverside, Riverside, CA 92521, USA

[d] Materials Science Division, Argonne National Laboratory, 9700 S. Cass Avenue, Lemont, IL 60439, USA

[e] Department of Chemical Engineering, University of Illinois at Chicago, Chicago, Illinois 60608, USA

[f] Material Science and Engineering, Stanford University, Stanford, CA 94305, USA

*E-mail: csu@anl.gov; amine@anl.gov

## ABSTRACT

To facilitate the practical application of lithium metal batteries (LMBs), stable interfaces between the electrolyte and the lithium metal must be achieved. Herein, we introduce a solvation protection strategy for designing a functional electrolyte for high-voltage LMBs. Fluoroethylene carbonate (FEC) was introduced as a solvation protection solvent for the difluoroethylene carbonate (DFEC)/trifluoroethyl methyl carbonate (FEMC) electrolyte system to enable the cycling of lithium metal anode. The addition of FEC alters the structures of lithium complexes in solution because of its relatively high solvating power. Through the precise control of the solvation number (> 1) of fluorinated cyclic carbonate (*i.e.*, FEC:DFEC > critical ratio), lithium complexes with $Li^+$ solvated solely by FEMC, which decompose on

the lithium surface to form detrimental by-products, can be effectively eliminated. The new ternary FEC/DFEC/FEMC system not only maintains the beneficial effect of DFEC in forming a robust solid-electrolyte interphase on the lithium anode, but also confers outstanding anodic stability provided by FEMC, while eliminating detrimental FEMC decomposition through the solvation protection effect of FEC. Clearly, this ternary system outperforms the FEC/FEMC and DFEC/FEMC binary systems in facilitating the stable cycling of LMBs.

## TOC Graphic

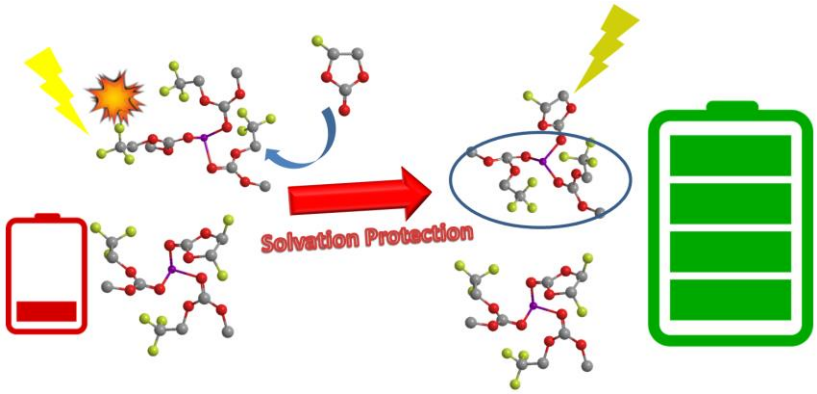


## Introduction

The remarkably high energy density delivered by a lithium metal anode and high-voltage layered oxide cathode renders high-voltage lithium metal batteries (LMBs) one of the most prominent potential candidates for next-generation battery systems. [1-5] However, the commercialization of LMBs is still impeded by their limited battery lives and severe safety issues arising from the high reactivity of lithium metal, [4-9] as well as the very unstable interfaces between electrolytes and the lithium anode. [9-11] To stabilize the lithium metal, researchers have been actively pursuing new approaches such as artificial protective layers on the lithium anode [12-14] and solid-state electrolytes. [14-16] Among the proposed

methods, the development of functional electrolytes provides an easy and cost-effective way to tackle the problem. [17-20] Apparently, conventional electrolytes designed for lithium ion batteries are incapable of stabilizing the cycling of a lithium anode. [17-18,21] To worsen the situation, since the ethylene carbonate (EC)-based conventional electrolyte was originally tailored for 4-V lithium ion chemistry, it displays poor performance in high-voltage ($\geq$ 4.4 V vs. $Li/Li^+$) systems. [22-25] As a result, several novel EC-free electrolyte systems, such as super-concentrated [18, 26-28] and localized concentrated [29-30] electrolytes, were developed to specifically target the stabilization of the lithium metal anode. Among the newly proposed systems, fluorinated electrolyte is one of the most promising candidates for high-voltage LMBs, thanks to its intrinsic anodic stability [22, 31-34] and its ability to stabilize lithium plating/stripping through the formation of a lithium fluoride-rich solid-electrolyte interphase (SEI). [20-21,35-37] Since fluorinated solvents display reduced lithium-solvating ability [38-40] and increased reduction potential [22, 38-42] compared to their non-fluorinated counterparts, the protocol for electrolyte design for fluorinated electrolytes is also different. [38-40, 43] For example, the fluorinated solvent methyl(2,2,2-trifluoroethyl) carbonate (FEMC), which exhibits significantly improved high-voltage stability, should be adopted cautiously because of its reduced reduction stability. [38-40] Unlike its non-fluorinated counterpart ethyl methyl carbonate (EMC), difluoroethylene carbonate (DFEC) is not desirable for use in FEMC-based electrolytes, although DFEC enables excellent SEI formation on the lithium anode in EMC-based electrolytes. [37, 39] The relatively high reduction potential of FEMC may induce severe decomposition of FEMC if a significant amount of FEMC solely solvating lithium complexes are presented in the electrolyte. [39] To fully utilize the advantages provided by fluorinated solvents, we herein propose a new strategy utilizing the solvation protection of fluoroethylene carbonate (FEC), which possesses significantly higher lithium-solvating power than DFEC, [39] to eliminate any lithium aggregates solvated solely by FEMC and “protect” the lithium anode from the detrimental by-

products generated by the decomposition of FEMC. When a significant amount of FEC is introduced into an electrolyte comprising DFEC and FEMC, the resulting ternary electrolyte not only possesses very high anodic stability, but also enables the formation of an excellent SEI induced by DFEC that suppresses the formation of lithium dendrites and eliminates the adverse interference from the reductive decomposition of FEMC. Li||$LiNi_{0.8}Mn_{0.1}Co_{0.1}O_2$ (NMC811) cells employing 1.2M lithium hexafluorophosphate ($LiPF_6$) in FEC/DFEC/FEMC electrolytes displayed very stable cycling performance when the volume ratio of FEC to DFEC was > 1, owing to the removal of lithium aggregates solely solvated by FEMC.

## Results and Discussion

To begin, FEMC is commonly used as a fluorinated co-solvent to facilitate high-voltage operation of lithium batteries. [23,43-44] Figures 1a and 1b present, respectively, the capacity retention and Coulombic efficiency (CE) of Li||NMC811 cells using FEC/EMC and FEC/FEMC electrolytes cycled between 3.0 V and 4.4 V; the cycling details are summarized in Table S1. Obviously, the FEMC cell outperformed the EMC cell, with significantly higher capacity retention and average CE under high-voltage cycling, owing not only to the enhanced anodic stability of FEMC but also to the reduced solvating ability towards metal ions. [45] In our previous study, we demonstrated that DFEC displayed superior lithium-stabilization capability, even better than that of FEC, in EMC-based electrolyte. [37] Yet, DFEC was found to be incompatible with FEMC-based electrolyte for LMBs. [39] Hence, it is highly desirable to solve the compatibility problem and incorporate the beneficial effects of both DFEC and FEMC in one electrolyte.

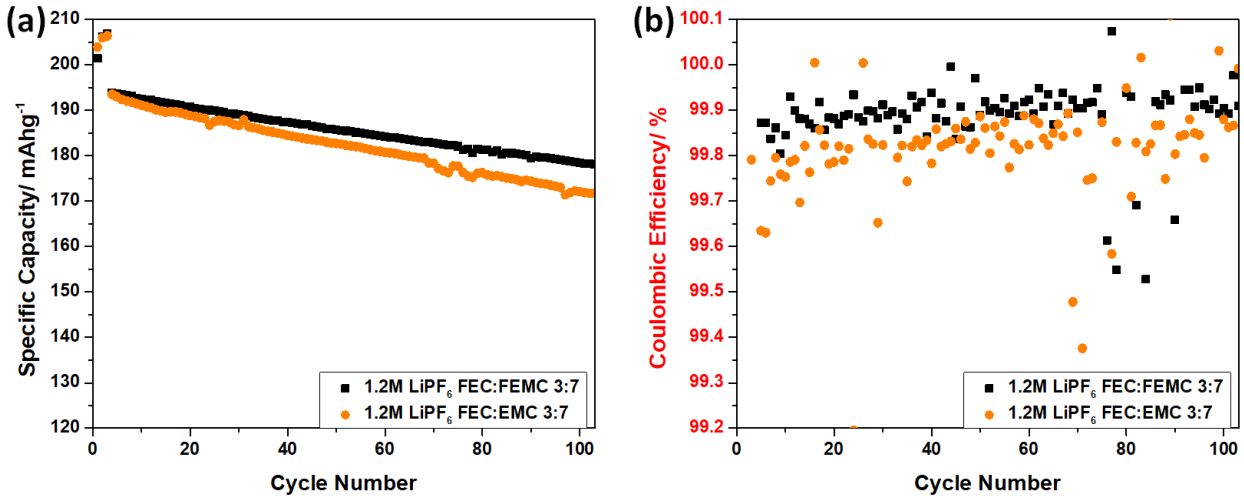


Figure 1. (a) Cycling performance and (b) Coulombic efficiency of Li||NMC811 cells using 1.2M $LiPF_6$-FEC/EMC and FEC/FEMC electrolytes.

The efficiency of lithium plating/stripping enabled by FEMC-based fluorinated electrolytes was evaluated by a Li||Cu cell test. [29, 37] Figure 2a presents an exemplary voltage profile and average 10-cycle CE of the Li||Cu cell using 1.2M $LiPF_6$ in FEC:DFEC:FEMC 3:3:14 (V:V:V) electrolyte; the voltage profiles of Li||Cu cells using electrolytes with other ratios are displayed in Figures S1-S4. The average CE remains at around 98.5% when the ratio of DFEC to total DFEC and FEC lies between 0 and 0.5, and it drops to around 97.5% when the ratio is > 0.5 (Figure 2b), indicating that a significant amount of FEC (FEC > DFEC) enabled a more stable lithium plating/stripping process. Moreover, the difficulty of charge transfer on the lithium anode was assessed by the exchange current density $i_0$ obtained from Tafel plots of Li||Li cells using various FEC/DFEC/FEMC electrolytes, which are displayed in Figure 2c. [46-47] As depicted in Figure 2d, the calculated $i_0$ values decreased upon the decrease of the DFEC ratio until the volume ratio of DFEC = FEC, and the $i_0$ values remained the same after the volume ratio of FEC > DFEC. This result agrees with the finding of the Li||Cu cell test, which suggests the formation of a more

robust SEI on the lithium surface after FEC reaches a critical ratio. Figure S5 depicts the Li||Li cell test for different electrolyte systems. The voltage fluctuation and polarization of the cells using DFEC:FEMC 3:7 and DFEC:FEC:FEMC 5:1:14 electrolytes are relatively high. On the contrary, the cells using FEC-FEMC and DFEC-FEC-FEMC (FEC >DFEC) electrolytes displayed lowered polarization and stabilized within 10 cycles. Clearly, the results of both Li||Li and Li||Cu cell tests all point to the enhancement of lithium plating/stripping stability and the mitigation of lithium dendrite formation when the addition of FEC is beyond the critical ratio.

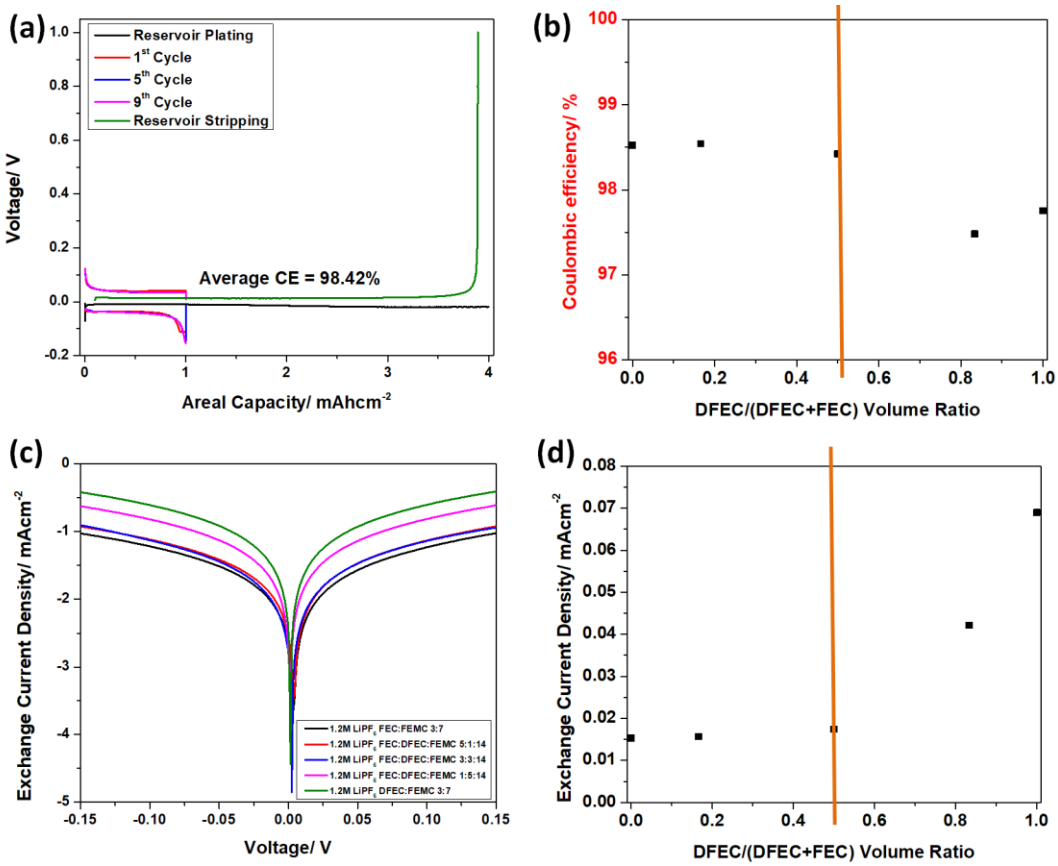


Figure 2. (a) Voltage profile of Li plating/stripping using Li||Cu cell with 1.2M $LiPF_6$-FEC:DFEC:FEMC 3:3:14 electrolyte; (b) Coulombic efficiency versus the ratio of DFEC:(DFEC + FEC) for the Li plating/stripping using

Li||Cu cells with 1.2M $LiPF_6$-FEC/DFEC/FEMC electrolyte; (c) Tafel plots obtained from cyclic voltammetry test in Li||Li cells with various 1.2M $LiPF_6$-FEC/DFEC/FEMC electrolytes; and (d) exchange current density vs. the ratio of DFEC:(DFEC + FEC).

A series of solvation studies were carried out to reveal the mechanism behind the ultra-stable lithium plating/stripping after the volume ratio of FEC > DFEC. As displayed in Figure S6, the absorptions of FEC, DFEC, and FEMC in their Fourier-transform infrared (FTIR) spectra severely overlap with one another, rendering deconvolution of individual peaks impossible. However, the proton nuclear magnetic resonance ($^1$H-NMR) peaks of the three molecules can be easily distinguished in the $^1$H-NMR spectrum displayed in Figure S7. Thus, the solvation state of individual solvents in the FEC/DFEC/FEMC ternary electrolyte system with different DFEC:FEC ratios can be easily determined by internally referenced diffusion-ordered spectroscopy (IR-DOSY). [39, 48] Table S2 summarizes the molar ratio of individual solvents in electrolytes with various DFEC:FEC volume ratios. Figures 3a and 3b display, respectively, the $^1$H-DOSY spectra of FEC:DFEC:FEMC 3:3:14 (critical FEC:DFEC 1:1 ratio) with and without the addition of $LiPF_6$. Apparently, the diffusion coefficients of FEC and DFEC are very similar and slightly larger than that of FEMC before the addition of $LiPF_6$. After the addition of $LiPF_6$, FEC diffuses the most slowly while DFEC diffuses the fastest, indicating that a significantly higher percentage of FEC is coordinating with lithium cations. With the use of toluene as an internal reference, the coordination ratio, solvation number (SN), and coordination number of FEC, DFEC and FEMC can be easily determined, [48] and the results are summarized in Table S3. Also performed were IR-DOSY studies on electrolytes with FEC:DFEC:FEMC ratios of 1:5:14 and 5:1:14, while the corresponding $^1$H-DOSY spectra are shown in Figures S8 and S9. Tables S4 and S5 also summarize, respectively, the solvation details of FEC:DFEC:FEMC 1:5:14 and 5:1:14 electrolytes. For the $LiPF_6$ in FEC/DFEC/FEMC electrolytes with three different ratios, the coordination ratios of the solvents follow the order FEC > FEMC > DFEC, and the coordination number of lithium increases slightly upon the increase of the FEC ratio. This is

consistent with order of the solvating power FEC (0.63) > FEMC (0.44) > DFEC (0.10) as demonstrated in our previous work. [39] From the structural perspective, the solvating power of FEC is higher than that of FEMC since it is a cyclic carbonate. For the case of DFEC, it has two electron withdrawing fluorine atoms locating on both side of the carbonate, largely reduced the solvating ability of the carbonyl oxygen. Since a solvent molecule coordinating to the positively charged lithium ion reduces much more readily than a non-coordinating one, it is crucial to determine the SN of an individual solvent, which is the average number of molecules associated with one lithium cation. The SNs of FEC, DFEC and FEMC in different electrolytes are calculated and presented in Table 1. Noticeably, the SN of FEMC drops slightly upon the increase of the FEC:DFEC ratio, while it remains close to 2, suggesting that there are, on average, two FEMC molecules coordinating with lithium cations in the solvated lithium complexes. Notably, the total SN of cyclic carbonates ($SN_{tc}$), which is the sum of the SNs of FEC and DFEC, increases significantly upon the rise of the FEC:DFEC ratio. For the electrolyte with FEC:DFEC in a 1:5 ratio, the $SN_{tc}$ is 0.90 < 1, implying the prevalence of lithium complexes being solvated solely by the linear fluorinated carbonate FEMC in the solution. However, when the FEC:DFEC ratio > 1:1, the $SN_{tc}$ is significantly larger than 1, indicating that at least one cyclic carbonate molecule, either FEC or DFEC, is solvating the lithium cation in the lithium complexes (including separated ion pairs, contact ion pairs, and lithium aggregates). As reported previously, the decomposition of FEMC on a lithium metal anode, which leads to the formation of methoxide or trifluoroethoxide and carbonates, is highly detrimental for the lithium metal cell because the decomposition by-products not only react with electrolyte solvents, but also impair the robust SEI formed by the reduction of FEC or DFEC. [39] On the contrary, the sacrificial decomposition of FEC or DFEC is able to continuously “repair” the SEI on the lithium anode, which can be easily damaged upon long-term cycling. [37, 39] Since the lowest unoccupied molecular orbital (LUMO) of FEC- or DFEC-containing lithium complexes is located on the cyclic carbonate, [39] the

presence of FEC or DFEC in the lithium complexes can "protect" against the decomposition of FEMC, which is highly deleterious to the cycling of the lithium anode. Therefore, the addition of FEC to the DFEC/FEMC electrolyte beyond the critical FEC:DFEC (1:1) ratio can provide an effective "solvation protection" effect, suppressing the detrimental decomposition of FEMC by eliminating lithium complexes solely solvated by FEMC. Although the critical FEC:DFEC ratio may vary slightly upon the change of the ratio between total cyclic carbonates and FEMC, the solvation protection effect is only present when FEC is added beyond the critical FEC:DFEC ratio, at which $SN_{tc}$ of the all-fluorinated electrolyte is significantly larger than 1. This postulation is further validated by density functional theory calculations that reveal the LUMO level of an FEMC molecule in electrolytes with distinctive FEC:DFEC ratios. The unit cells representing 1.2M $LiPF_6$ dissolved in FEC:DFEC:FEMC with volume ratios 1:5:14 and 5:1:14 are depicted in Figure S10, while the projected density of states of optimized structures of FEMC in the two different electrolytes are presented in Figure 4. Accordingly, the energy level of FEMC in the electrolyte with FEC:DFEC ratio exceeding the critical ratio (FEC:DFEC 5:1 > 1:1) is considerably higher (0.5 eV higher) than the energy level in the electrolyte with FEC:DFEC smaller than the critical ratio (FEC:DFEC 1:5 < 1:1), strongly suggesting that the FEMC molecule is much more resistant to reduction in the electrolyte with an FEC:DFEC ratio exceeding the critical ratio. In summary, this ternary FEC/DFEC/FEMC electrolyte system with FEC:DFEC larger than the critical ratio offers an exceptionally stable high-voltage electrolyte for LMBs by combining the beneficial effect of DFEC, which is able to form a highly stable SEI on the lithium anode, and the advantage of using FEMC, which delivers extraordinary anodic stability, while eliminating the detrimental FEMC decomposition through the solvation protection effect of FEC.

To further corroborate the solvation protection effect of FEC, we performed X-ray photoelectron spectroscopy (XPS) analysis on the lithium anode of Li||NMC811 cells employing various all-fluorinated

electrolytes after 3 formation cycles. The C1s, F1s, O1s and P2p XPS spectra of the lithium anodes from the cells using FEC:DFEC:FEMC 5:1:14, FEC:FEMC 3:7, and DFEC:FEMC 3:7 electrolytes are depicted, respectively, in Figures S11a, S11b and S11c. Qualitatively, the FEC/DFEC/FEMC cell shares more similar C1s, O1s and P2p spectra with the DFEC/FEMC cell than the FEC/FEMC cell, suggesting that DFEC is actively participating in the formation of SEI on the lithium anode in the FEC/DFEC/FEMC cell. Most importantly, the presence of a $CF_3$ group in the C1s spectrum of the lithium anode from the DFEC/FEMC cell, which can only originate from the decomposition of FEMC, illustrates the inability of the DFEC/FEMC electrolyte to mitigate the reduction of FEMC. On the contrary, no absorption peak from the $CF_3$ group was observed in the C1s spectra of FEC/FEMC and FEC/DFEC/FEMC cells, signaling that the lithium anode was "protected" from FEMC decomposition. Evidently, the addition of FEC to DFEC/FEMC electrolyte provides solvation protection to the lithium anode by suppressing the decomposition of FEMC through its preferential solvating ability towards the lithium cation.

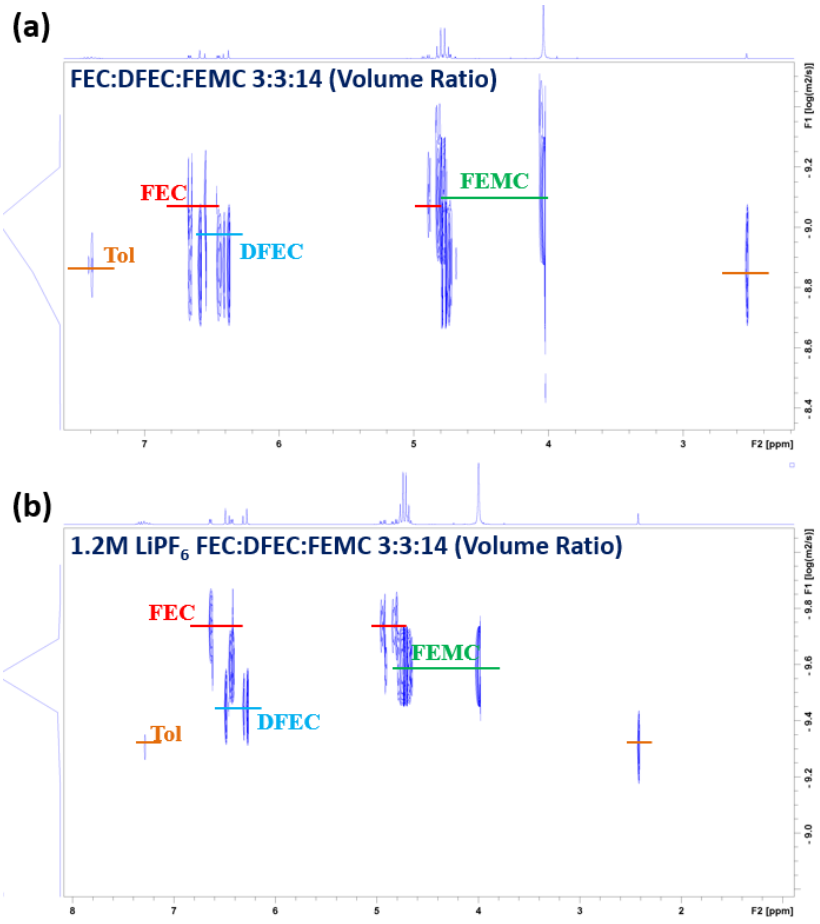


Figure 3. $^{1}$H DOSY-NMR spectra of (a) FEC:DFEC:FEMC 3:3:14 (V:V:V) electrolyte and (b) 1.2M $LiPF_6$-FEC:DFEC:FEMC 3:3:14 (V:V:V) electrolyte, with toluene added as an internal reference.

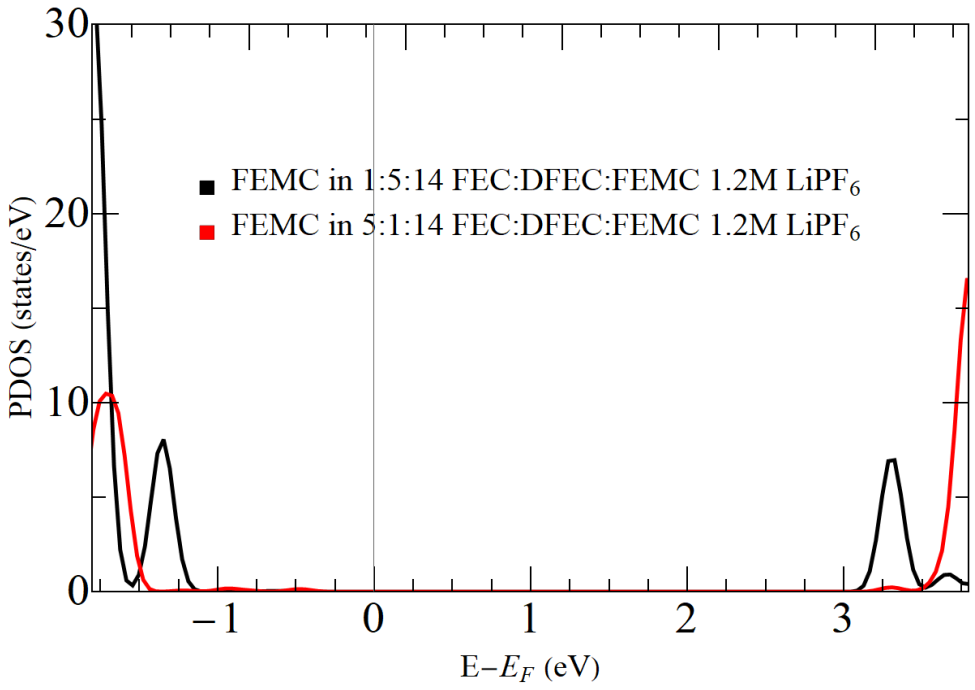


Figure 4. Projected density of states (PDOS) of FEMC obtained in DFT simulations on 1.2M $LiPF_6$-FEC:DFEC:FEMC 1:5:14 and 1.2M $LiPF_6$-FEC:DFEC:FEMC 5:1:14 electrolytes.

Table 1. Coordination ratio (α) and solvation number (SN) of FEC, DFEC and FEMC in 1.2M $LiPF_6$-FEC/DFEC/FEMC electrolytes.

| Electrolyte | $\alpha_{FEC}$ | $\alpha_{DFEC}$ | $\alpha_{FEMC}$ | SN of FEC[a] | SN of DFEC[a] | SN of FEMC[a] | SN of Cyclic Carbonates (FEC+DFEC) |
|---|---|---|---|---|---|---|---|
| 1.2M $LiPF_6$-FEC:DFEC:FEMC 1:5:14 (V:V:V) | 0.65 | 0.22 | 0.47 | 0.36 | 0.54 | 2.23 | 0.90 |
| 1.2M $LiPF_6$-FEC:DFEC:FEMC 3:3:14 (V:V:V) | 0.63 | 0.15 | 0.44 | 1.07 | 0.21 | 2.05 | 1.28 |
| 1.2M $LiPF_6$-FEC:DFEC:FEMC 5:1:14 (V:V:V) | 0.60 | 0.26 | 0.44 | 1.59 | 0.13 | 1.95 | 1.72 |

[a] Solvation numbers of FEC, DFEC and FEMC were calculated by multiplying the coordination ratios of solvents with their solvent-to-lithium molar ratios.

The practical application of this solvation protection strategy can be clearly demonstrated by the electrochemical performance of Li||NMC811 cells. Firstly, the performance of high voltage NMC cell was affected heavily by the anodic stability of the electrolyte and thus, it is important to evaluate the oxidation stability of the all-fluorinated electrolytes. As expected, all the FEC/DFEC/FEMC electrolytes possess exceptional anodic stability, evidenced by the linear sweep voltammograms of 1.2M $LiPF_6$-FEC/DFEC/FEMC electrolytes with different FEC to DFEC ratios displayed in Figure S12. The onset oxidation voltages for all the fluorinated electrolytes were larger than 7.2 V, which is significantly higher than the upper cutoff voltage (4.4 V) of the Li||NMC811 cells. Therefore, all of the fluorinated electrolytes are highly stable towards the NMC811 cathode. Moreover, the conductivities of various1.2M $LiPF_6$-FEC/DFEC/FEMC electrolytes were presented in Table S6. The conductivity of the fluorinated electrolytes increases with the rise of FEC content. Yet, the conductivities of all the electrolytes are larger than 3 mS/cm, which is adequate for the cycling of the Li||NMC811 cells. The cycling performance of Li||NMC811 cells was illustrated in Figures 5a and 5b, which respectively display the capacity retention and CE of Li||NMC811 cells using FEC/DFEC/FEMC electrolytes with various FEC:DFEC ratios, while the cycling details are summarized in Table 2. The Li||NMC811 cells were cycled at a rate of C/2 with a cutoff voltage between 4.4 and 3.0 V, following 3 formation cycles at a rate of C/10. Clearly, the cell employing DFEC/FEMC electrolyte showed inferior cycling performance, evidenced by its sudden rapid capacity drop starting at around the $20^{th}$ cycle. The addition of a small amount of FEC to the DFEC/FEMC electrolyte, giving a FEC:DFEC ratio of 1:5, provided very little protective effect, and the cell using the FEC:DFEC:FEMC 1:5:14 electrolyte still experienced a sudden rapid drop of capacity during early cycling, at around the $30^{th}$ cycle. However, the cycling performance of the Li||NMC811 cell was enhanced drastically when the FEC:DFEC ratio exceeded the critical ratio (1:1) with $SN_{tc}$ larger than 1. The Li||NMC811 cells with FEC:DFEC:FEMC 3:3:14 and FEC:DFEC:FEMC 5:1:14 electrolytes

showed similarly highly stable cycling performance, with average CEs around 99.8% for the first 50 cycles. In comparison, the DFEC:FEMC 3:7 and FEC:DFEC:FEMC 1:5:14 cells displayed not only significantly lower first-50-cycle average CEs, but also extremely unstable cycling performance due to the insufficient solvation protection by FEC. Although the Li||NMC811 cell using electrolyte without DFEC (FEC:FEMC 3:7) also showed stable cycling capability, the long-term performance of the FEC/FEMC cell was not as outstanding as that of the FEC/DFEC/FEMC cells with FEC:DFEC larger than the critical ratio; this finding was supported by the fact that the average 200-cycle capacity retention of the FEC/FEMC cell (82.6 %) was significantly lower than that of the cell using FEC:DFEC:FEMC 3:3:14 electrolyte (90.8 %). Figures S13a, S13b, S13c and S13d exhibited respectively the $1^{st}$-cycle, $5^{th}$-cycle, $50^{th}$-cycle and $200^{th}$-cycle voltage profiles of the Li||NMC811 cells using various 1.2M $LiPF_6$-FEC/DFEC/FEMC electrolytes. The cell employing electrolyte without DFEC (FEC-FEMC) showed significantly higher polarization in the $1^{st}$ cycle than all the cells using electrolytes with DFEC. However, the polarizations of the cells using electrolytes with FEC:DFEC lower than the critical ratio (*i.e.* DFEC:FEMC 3:7 and DFEC:FEC:FEMC 5:1:14 electrolytes) increased drastically, displaying significantly higher polarization than the FEC-FEMC cell. Apparently, the cells using ternary electrolytes with FEC:DFEC > critical ratio (*i.e.* DFEC:FEC:FEMC 3:3:14 and DFEC:FEC:FEMC 1:5:14 electrolytes) experienced the least increase in the cell polarization. Again, the results of these cycling tests strongly coincide with our previous finding that the ternary FEC/DFEC/FEMC electrolyte system becomes a superior high-voltage electrolyte for LMBs through the solvation protection effect of FEC when the FEC:DFEC ratio is larger than the critical ratio.

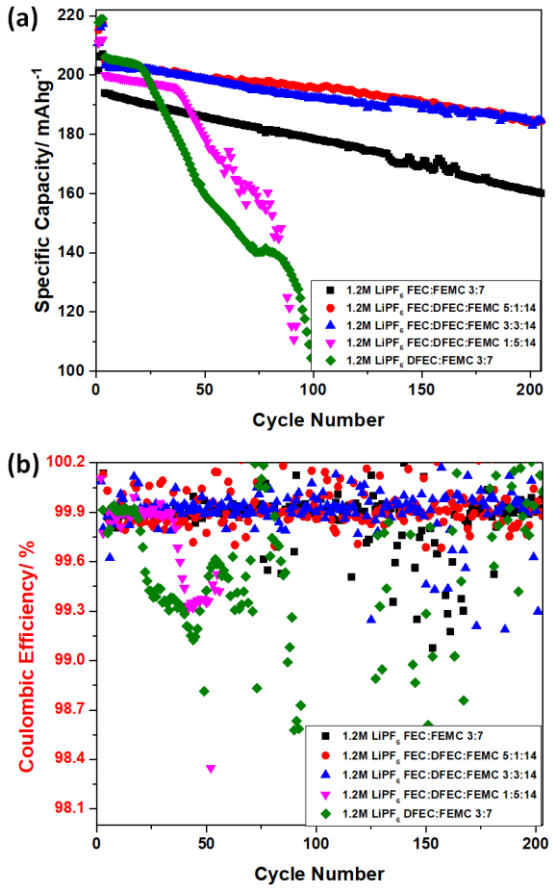


Figure 5. (a) Cycling performance and (b) Coulombic efficiency of Li||NMC811 cells using 1.2M $LiPF_6$-FEC/DFEC/FEMC in different ratios.

Table 2. Data associated with Figure 5 for Li||NMC811 cell operated at voltage range of 3.0–4.4 V with 1.2M $LiPF_6$-FEC/DFEC/FEMC electrolytes in different FEC:DFEC:FEMC ratios: $1^{st}$-cycle Coulombic efficiency ($1^{st}$ CE), $1^{st}$-cycle discharge capacity ($1^{st}$ DC), capacity retention after 200 cycles (CR-200), average CE of 200 cycles (ACE-200), and average CE of 50 cycles (ACE-50).

| Electrolyte | $1^{st}$ CE | $1^{st}$ DC (mAh/g) | CR-200 | ACE-200 | ACE-50 |
|---|---|---|---|---|---|
| 1.2M $LiPF_6$ DFEC:FEMC 3:7 (V:V) | 91.3% | 217.7 | - | - | 99.45% |
| 1.2M $LiPF_6$ | 91.8% | 210.8 | - | - | 99.59% |

| | | | | | |
|---|---|---|---|---|---|
| FEC:DFEC:FEMC 1:5:14 (V:V:V) | | | | | |
| 1.2M $LiPF_6$ FEC:DFEC:FEMC 3:3:14 (V:V:V) | 90.1% | 210.9 | 90.8% | 99.91% | 99.81% |
| 1.2M $LiPF_6$ FEC:DFEC:FEMC 5:1:14 (V:V:V) | 88.4% | 215.2 | 90.2% | 99.90% | 99.80% |
| 1.2M $LiPF_6$ FEC:FEMC 3:7 (V:V) | 89.0% | 201.4 | 82.6% | 99.87% | 99.78% |

## Conclusion

In summary, a solvation protection strategy was established to construct high-voltage fluorinated electrolytes for LMBs. Owing to the relatively high solvating power of FEC, it was introduced into the DFEC/FEMC electrolyte to serve as a solvation protection agent. The results of cell testing and advanced solvation studies clearly indicated that when the addition of FEC exceeded the critical FEC:DFEC ratio, at which the total SN of cyclic carbonates is larger than 1, FEMC was "protected" from decomposition. This new ternary FEC/DFEC/FEMC electrolyte system with FEC:DFEC larger than the critical ratio evidently enables exceptional cycling of Li||NMC811 cells by combining the outstanding SEI formation ability of DFEC and the superior anodic stability of FEMC, while mitigating the deleterious effect of FEMC decomposition through the solvation protection effect of FEC. As a result, this solvation protection strategy represents a powerful approach for the re-design of functional electrolyte systems.

## ASSOCIATED CONTENT

**Supporting Information**

Experimental section, supplementary electrochemical data, NMR data, FTIR data and supplementary tables. This material is available free of charge via the Internet.

## AUTHOR INFORMATION

**Corresponding Author**

*Email: csu@anl.gov; amine@anl.gov

**Notes**

The authors declare no competing financial interest.

## ACKNOWLEDGMENTS

This work was conducted as part of the U.S.-German joint collaboration on "Interfaces and Interphases In Rechargeable Li-metal Based Batteries" supported by the U.S. Department of Energy (DOE) and the German Federal Ministry of Education and Research (BMBF). Financial support was provided by the U.S. Department of Energy (DOE), Vehicle Technologies Office (VTO). Argonne National Laboratory is operated for the DOE Office of Science by UChicago Argonne, LLC, under contract number DE-AC02-06CH11357 under the U.S.-Germany Cooperation on Energy Storage. The NMC811 electrodes were manufactured at the DOE's CAMP Facility at Argonne National Laboratory. The CAMP Facility is fully supported by the DOE VTO within the core funding of the Applied Battery Research for Transportation Program. We gratefully acknowledge the computer time from the Argonne National Laboratory Computing Resource Center (LCRC). The authors also thank Kris Pupek and Gregory Krumdick from Argonne's Materials Engineering Research Facility (MERF) for supplying FEMC solvent.

## REFERENCES


1. Fang, C.; Li, J.; Zhang, M.; Zhang, Y.; Yang, F.; Lee, J. Z.; Lee, M. H.; Alvarado, J.; Schroeder, M. A.; Yang, Y.; Lu, B.; Williams, N.; Ceja, M.; Yang, L.; Cai, M.; Gu, J.; Xu, K.; Wang, X.; Meng, Y. S., *Nature* **2019**, *572*, 511.
2. Fang, C.; Wang, X.; Meng, Y. S., *Trends in Chemistry* **2019**, *1 (2)*, 152–158.
3. Lin, D.; Liu, Y.; Cui, Y., *Nature Nanotechnology* **2017**, *12*, 194.
4. Li, S.; Jiang, M.; Xie, Y.; Xu, H.; Jia, J.; Li, J., *Advanced Materials* **2018**, *30* (*17*), e1706375.
5. Cheng, X. B.; Zhang, R.; Zhao, C. Z.; Zhang, Q., *Chemical Reviews* **2017**, *117* (*15*), 10403–10473.
6. Doron, A.; Zinigrad, E.; Cohen, Y.; Teller, H., *Solid State Ionics* **2002**, *148*, 405–416.
7. Li, X.; Zheng, J.; Ren, X.; Engelhard, M. H.; Zhao, W.; Li, Q.; Zhang, J.-G.; Xu, W., *Advanced Energy Materials* **2018**, *8* (*15*), 1703022.
8. Liang, X.; Pang, Q.; Kochetkov, I. R.; Sempere, M. S.; Huang, H.; Sun, X.; Nazar, L. F. *Nature Energy* **2017**, *2* (9), 17119.
9. Xu, W.; Wang, J.; Ding, F.; Chen, X.; Nasybulin, E.; Zhang, Y.; Zhang, J.-G., *Energy Environ. Sci.* **2014**, *7* (2), 513.
10. Zheng, J.; Yan, P.; Mei, D.; Engelhard, M. H.; Cartmell, S. S.; Polzin, B. J.; Wang, C.; Zhang, J.-G.; Xu, W. *Adv. Energy Mater.* **2016**, *6* (8), 1502151.
11. Zhou, Q.; Dong, S.; Lv, Z.; Xu, G.; Huang, L.; Wang, Q.; Cui, Z.; Cui, G., *Advanced Energy Materials* **2019**, *10* (*6*), 1903441.
12. Zhou, H.; Yu, S.; Liu, H.; Liu, P., *Journal of Power Sources* **2020**, *450*, 227632.
13. Liang, X.; Pang, Q.; Kochetkov, I. R.; Sempere, M. S.; Huang, H.; Sun, X.; Nazar, L. F. *Nature Energy* **2017**, *2* (9), 17119.
14. Xu, R.; Cheng, X.-B.; Yan, C.; Zhang, X.-Q.; Xiao, Y.; Zhao, C.-Z.; Huang, J.-Q.; Zhang, Q., *Matter* **2019**, *1 (2)*, 317.
15. Liu, Y.; Lin, D.; Yuen, P. Y.; Liu, K.; Xie, J.; Dauskardt, R. H.; Cui, Y., *Advanced Materials* **2017**, *29,* 1605531.
16. Li, N. W.; Yin, Y. X.; Yang, C. P.; Guo, Y. G. *Advanced Materials* **2016**, *28* (9), 1853.
17. Xiang, H.; Shi, P.; Bhattacharya, P.; Chen, X.; Mei, D.; Bowden, M. E.; Zheng, J.; Zhang, J.-G.; Xu, W., *J. Power Sources* **2016**, *318*, 170.
18. Wang, J.; Yamada, Y.; Sodeyama, K.; Watanabe, E.; Takada, K.; Tateyama, Y.; Yamada, A., *Nature Energy* **2017**, *3* (1), 22.
19. Suo, L.; Xue, W.; Gobet, M.; Greenbaum, S. G.; Wang, C.; Chen, Y.; Yang, W.; Li, Y.; Li, J., *PNAS* January **2018**, 201712895.

20. Salitra, G.; Markevich, E.; Afri, M.; Talyosef, Y.; Hartmann, P.; Kulisch, J.; Sun, Y. K.; Aurbach, D., *ACS Applied Materials & Interfaces* **2018**, *10* (23), 19773.
21. He, M.; Su, C.-C.; Xu, F.; Amine, K.; Cai, M., *ACS Applied Materials & Interfaces* **2021**, *13* (22), 25879.
22. He, M.; Su, C.-C.; Feng, Z.; Zeng, L.; Wu, T.; Bedzyk, M. J.; Fenter, P.; Wang, Y.; Zhang, Z., *Advanced Energy Materials* **2017**, *7* (15), 1700109.
23. Xu, K., *Chem. Rev.*, **2014**, *114*, 11503.
24. Xu, M.; Zhou, L.; Dong, Y.; Chen, Y.; Demeaux, J.; Macintosh, A. D.; Garsuch, A.; Lucht, B. L., *Energy Environ. Sci.*, **2016**, *9*, 1308.
25. Xia, J.; Petibon, R.; Xiong, D.; Ma, L.; Dahn, J., *J. Power Sources* **2016,** *328*, 124.
26. Zheng, J.; Lochala, J. A.; Kwok, A.; Deng, Z. D.; Xiao, J., *Advanced Science* **2017**, *4* (8), 1700032.
27. Wang, J.; Yamada, Y.; Sodeyama, K.; Chiang, C. H.; Tateyama Y.; Yamada, A., *Nature Commun*. **2016**, *7*, 2032.
28. Alvarado, J.; Schroeder, M. A.; Zhang, M.; Borodin, O.; Gobrogge, E.; Olguin, M.; Ding, M. S.; Gobet, M.; Greenbaum, S.; Meng, Y. S.; Xu, K., *Materials Today* **2018**, *21* (4), 341.
29. Chen, S.; Zheng, J.; Mei, D.; Han, K. S.; Engelhard, M. H.; Zhao, W.; Xu, W.; Liu, J.; Zhang, J. G., *Adv. Mater.* **2018**, *30* (21), e1706102.
30. Yu, L.; Chen, S.; Lee, H.; Zhang, L.; Engelhard, M. H.; Li, Q.; Jiao, S.; Liu, J.; Xu, W.; Zhang, J.-G., A *ACS Energy Letters* **2018**, *3 (9)*, 2059.
31. Xu, K., *Chem. Rev.*, **2014**, *114*, 11503.
32. Chen, S.; Wen, K.; Fan, J.; Bando, Y.; Golberg, D., *Journal of Materials Chemistry A* **2018**, *6* (25), 11631.
33. Fan, X.; Chen, L.; Borodin, O.; Ji, X.; Chen, J.; Hou, S.; Deng, T.; Zheng, J.; Yang, C.; Liou, S. C.; Amine, K.; Xu, K.; Wang, C., *Nature Nanotechnology* **2018**, *13*, 715.
34. Su, C.-C.; He, M.; Redfern, P. C.; Curtiss, L. A.; Shkrob, I. A.; Zhang, Z., *Energy Environ. Sci.* **2017**, *10* (4), 900.
35. Markevich, E.; Salitra, G.; Chesneau, F.; Schmidt, M.; Aurbach, D., *ACS Energy Letters* **2017**, *2* (6), 1321.
36. Zhang, X.-Q.; Cheng, X.-B.; Chen, X.; Yan, C.; Zhang, Q., *Advanced Functional Materials* **2017**, *27* (10), 1605989.
37. Su, C.-C.; He, M.; Amine, R.; Chen, Z.; Sahore, R.; Dietz Rago, N.; Amine, K., *Energy Storage Materials*. **2019**, *17*, 284.
38. Su, C.-C.; He, M.; Shi, J.; Amine, R.; Rojas, T.; Cheng, L.; Ngo, A. T.; Amine, K., *Energy & Environmental Science* **2021**, *14*, 3029.
39. Su, C.-C.; He, M.; Amine, R.; Rojas, T.; Cheng, L.; Ngo, A. T.; Amine, K., *Energy & Environmental Science* **2019**, *12*, 1249.
40. Su, C.-C.; He, M.; Shi, J.; Amine, R.; Zhang, J.; Guo, J.; Amine, K., *Nano Energy* **2021**, *89*, 106299.

41. Lee, Y.-M.; Nam, K.-M.; Hwang, E.-H.; Kwon, Y.-G.; Kang, D.-H.; Kim, S.-S.; Song, S.-W., *J. Phys. Chem. C* **2014**, *118*, 10631.
42. Zhang, Z.; Hu, L.; Wu, H.; Weng, W.; Koh, M.; Redfern, P. C.; Curtiss, L. A.; Amine, K. *Energy Environ. Sci.* **2013**, *6* (6), 1806.
43. He, M.; Hu, L.; Xue, Z.; Su, C. C.; Redfern, P.; Curtiss, L. A.; Polzin, B.; von Cresce, A.; Xu, K.; Zhang, Z., *J. Electrochem. Soc.* **2015**, *162* (9), A1725.
44. He, M.; Su, C.-C.; Peebles, C.; Zhang, Z., *Journal of The Electrochemical Society* **2021**, *168* (1), 010505.
45. Su, C. C.; He, M.; Amine, R.; Chen, Z.; Amine, K., *Nano Energy* **2021,** *83*, 105843.
46. Zhao, Q.; Tu, Z.; Wei, S.; Zhang, K.; Choudhury, S.; Liu, X.; Archer, L. A., *Angew. Chem. Int. Ed.* **2018**, *57*, 992.
47. Zhang, X.-Q.; Chen, X.; Hou, L.-P.; Li, B.-Q.; Cheng, X.-B.; Huang, J.-Q.; Zhang, Q., *ACS Ener. Lett.* **2019**, *4*, 411.
48. Su, C. C.; He, M.; Amine, R.; Chen, Z.; Amine, K., *J. Phys. Chem. Letters* **2018**, *9* (13), 3714.

## KEYWORDS

High-voltage lithium metal batteries, fluorinated electrolyte, electrolyte solvation, solvation protection, solid-electrolyte interphase